TÜBİTAK

Turkish Journal of Mathematics

http://journals.tubitak.gov.tr/math/

Research Article

Turk J Math
(2022) 46: 2890 – 2901

doi:10.55730/1300-0098.3307

Nonic B-spline algorithms for numerical solution of the Kawahara equation

Melis ZORŞAHİN GÖRGÜLÜ*
Department of Mathematics and Computer Science, Faculty of Science and Letters,
Eskişehir Osmangazi University, Eskişehir, Turkey

Received: 07.01.2022 • **Accepted/Published Online:** 18.07.2022 • **Final Version:** 05.09.2022

Abstract: In this paper, the nonic (9th order) B-spline functions which have not been used before for the numerical solutions of the partial differential equations by finite element methods are used to solve numerically the Kawahara equation. These approaches involve the collocation and Galerkin finite element methods based on the nonic B-spline functions in space discretization and second order scheme (Crank-Nicolson method) in time discretization. To see the accuracy of the proposed methods three test problems are demonstrated and the obtained numerical results for both of the methods are compared with the exact solution of the Kawahara equation.

Key words: Collocation method, Galerkin method, nonic B-spline, Kawahara equation

1. Introduction

Many problems occurring in nature are modelled by partial differential equations (PDEs). In lots of physical phenomena in engineering, physics and applied sciences, the spline functions, which derived by Schoenberg [13] in 1946, have been widely used to get the numerical solutions of PDEs. DeBoor mentioned in his book [5] that the spline functions can be written as a linear combination of the B-spline functions. The B-spline functions of order k denoted by B_i^k are defined by the following recursive formula

$$B_i^k(x) = \frac{x - x_i}{x_{i+k} - x_i} B_i^{k-1}(x) + \frac{x_{i+k+1} - x}{x_{i+k+1} - x_{i+1}} B_{i+1}^{k-1}(x), \tag{1.1}$$

where

$$B_i^0(x) = \begin{cases} 1 & , \ x_i \le x < x_{i+1}, \\ 0 & , \ \text{otherwise}, \end{cases} \tag{1.2}$$

$k \ge 1$ and $i = 0, \pm 1, \pm 2, \ldots$. Since they have important geometric properties and lower computational costs, the B-splines known as base of the splines have been used for the numerical solutions of the PDE. The Kawahara equation (KE) which is in the standard form with the initial and boundary conditions

$$u_t + uu_x + u_{xxx} - u_{xxxxx} = 0, \tag{1.3}$$

*Correspondence:mzorsahin@ogu.edu.tr
2010 *AMS Mathematics Subject Classification:* 65M60, 65M70, 65D07, 76B25

$$u(x,0) = f(x), \tag{1.4}$$

$$\begin{aligned} u(c,t) &= \alpha_1, u(d,t) = \alpha_2, \\ u_x(c,t) &= \alpha_3, u_x(d,t) = \alpha_4, \\ u_{xx}(c,t) &= \alpha_5, u_{xx}(d,t) = \alpha_6, \\ u_{xxx}(c,t) &= \alpha_7, u_{xxx}(d,t) = \alpha_8, \\ u_{xxxx}(c,t) &= \alpha_9, u_{xxxx}(d,t) = \alpha_{10}, \end{aligned} \tag{1.5}$$

where $c \leq x \leq d$ and $t > 0$, is a nonlinear higher order PDE. Some physical phenomena which like as the magneto-acoustic waves in plasmas [10] and shallow water waves with surface tension [8] are modelled by Eq. (1.3). The way that the KE is of nonlinear and has fifth order derivative increases the difficulty to get the solution of the KE. Thus, various numerical methods [1, 3, 6, 9, 12, 14] have been presented before to get the numerical solutions of the KE.

In this paper, the numerical solution of the KE is presented by two different finite element methods which are the collocation method (CM) and the Galerkin method (GM). In both of two methods the nonic B-spline functions are used as weight and trial functions for space discretization and Crank-Nicolson method (CNM) is used for time discretization. What is considerable in this study is that the use of the high degree B-spline functions that have not been used before to solve numerically a high order partial differential equations. In Section 2, the time and space discretizations of the KE are explained. In Section 3, the solitary wave solution of KE, the interaction of the two solitary waves and the wave generation of the KE are tested to see the efficiency and the accuracy of the methods. The comparison of the obtained numerical solutions according to the error norms L_2 and L_∞ and conservative quantities are given with the tables.

2. Nonic B-spline finite element methods

The nonic B-spline functions at knots $x_r, r = 0, \ldots, N$ in the solution domain $[c,d]$ can be obtained using the recurrence relation (1.1) as

$$B_r^9(x) = \frac{1}{h^9} \begin{cases} \varphi_1 & , x_{r-5} \leq x < x_{r-4} \\ \varphi_2 & , x_{r-4} \leq x < x_{r-3} \\ \varphi_3 & , x_{r-3} \leq x < x_{r-2} \\ \varphi_4 & , x_{r-2} \leq x < x_{r-1} \\ \varphi_5 & , x_{r-1} \leq x < x_r \\ \varphi_6 & , x_r \leq x < x_{r+1} \\ \varphi_7 & , x_{r+1} \leq x < x_{r+2} \\ \varphi_8 & , x_{r+2} \leq x < x_{r+3} \\ \varphi_9 & , x_{r+3} \leq x < x_{r+4} \\ \varphi_{10} & , x_{r+4} \leq x < x_{r+5} \\ 0 & , \text{otherwise} \end{cases} \tag{2.1}$$

where

$$\begin{aligned}
\varphi_1 &= (x-x_{r-5})^9,\\
\varphi_2 &= h^9+9h^8(x-x_{r-4})+36h^7(x-x_{r-4})^2+84h^6(x-x_{r-4})^3\\
&\quad +126h^5(x-x_{r-4})^4+126h^4(x-x_{r-4})^5+84h^3(x-x_{r-4})^6\\
&\quad +36h^2(x-x_{r-4})^7+9h(x-x_{r-4})^8-9(x-x_{r-4})^9,\\
\varphi_3 &= 502h^9+2214h^8(x-x_{r-3})+4248h^7(x-x_{r-3})^2+4536h^6(x-x_{r-3})^3\\
&\quad +2772h^5(x-x_{r-3})^4+756h^4(x-x_{r-3})^5-168h^3(x-x_{r-3})^6\\
&\quad -216h^2(x-x_{r-3})^7-72h(x-x_{r-3})^8+36(x-x_{r-3})^9,\\
\varphi_4 &= 14608h^9+36414h^8(x-x_{r-2})+34272h^7(x-x_{r-2})^2+11256h^6(x-x_{r-2})^3\\
&\quad -4032h^5(x-x_{r-2})^4-4284h^4(x-x_{r-2})^5-672h^3(x-x_{r-2})^6\\
&\quad +504h^2(x-x_{r-2})^7+252h(x-x_{r-2})^8-84(x-x_{r-2})^9,\\
\varphi_5 &= 88234h^9+101934h^8(x-x_{r-1})+5544h^7(x-x_{r-1})^2-36456h^6(x-x_{r-1})^3\\
&\quad -10836h^5(x-x_{r-1})^4+5796h^4(x-x_{r-1})^5+2856h^3(x-x_{r-1})^6\\
&\quad -504h^2(x-x_{r-1})^7-504h(x-x_{r-1})^8+126(x-x_{r-1})^9,\\
\varphi_6 &= 156190h^9-88200h^7(x-x_r)^2+23940h^5(x-x_r)^4-4200h^3(x-x_r)^6\\
&\quad +630h(x-x_r)^8-126(x-x_r)^9,\\
\varphi_7 &= 88234h^9-101934h^8(x-x_{r+1})+5544h^7(x-x_{r+1})^2+36456h^6(x-x_{r+1})^3\\
&\quad -10836h^5(x-x_{r+1})^4-5796h^4(x-x_{r+1})^5+2856h^3(x-x_{r+1})^6\\
&\quad +504h^2(x-x_{r+1})^7-504h(x-x_{r+1})^8+84(x-x_{r+1})^9,\\
\varphi_8 &= 14608h^9-36414h^8(x-x_{r+2})+34272h^7(x-x_{r+2})^2-11256h^6(x-x_{r+2})^3\\
&\quad -4032h^5(x-x_{r+2})^4+4284h^4(x-x_{r+2})^5-672h^3(x-x_{r+2})^6\\
&\quad -504h^2(x-x_{r+2})^7+252h(x-x_{r+2})^8-36(x-x_{r+2})^9,\\
\varphi_9 &= 502h^9-2214h^8(x-x_{r+3})+4248h^7(x-x_{r+3})^2-4536h^6(x-x_{r+3})^3\\
&\quad +2772h^5(x-x_{r+3})^4-756h^4(x-x_{r+3})^5-168h^3(x-x_{r+3})^6\\
&\quad +216h^2(x-x_{r+3})^7-72h(x-x_{r+3})^8+9(x-x_{r+3})^9,\\
\varphi_{10} &= [h-(x-x_{r+4})]^9.
\end{aligned}$$

The set of nonic B-spline functions $\left\{B^9_{-4}(x), B^9_{-3}(x),\ B^9_{-2}(x),\ldots,\ B^9_{N+2}(x),\ B^9_{N+3}(x), B^9_{N+4}(x)\right\}$ generates a basis over the solution domain $[c,d]$.

Let the exact solutions of the unknown functions at the grid points be given as

$$u(x_r,t_s)=u^s_r,\ r=0,1,\ldots,N;\quad s=0,1,2,\ldots$$

where $x_r=c+rh,\ t_s=s\Delta t$ and the notation $U^s_r=U(x_r,t_s)$ is used to represent the numerical value of u^s_r.

Using CNM for the time discretization of Eq. (1.3), we have

$$u^{s+1}+\frac{\Delta t}{2}\left(uu_x^{s+1}+u_{xxx}^{s+1}-u_{xxxxx}^{s+1}\right)=u^s-\frac{\Delta t}{2}\left(uu_x^s+u_{xxx}^s-u_{xxxxx}^s\right). \tag{2.2}$$

2.1. Nonic B-spline collocation method (M1)

To set up the space discretization of Eq. (2.2), let us take the approximate solution U in terms for the nonic B-splines as

$$U(x,t)=\sum_{l=-4}^{N+4}B_l^9(x)\,\delta_l(t)\ , \tag{2.3}$$

where δ_l are time dependent unknowns which will be calculated. From (2.1), the each element $[x_r,x_{r+1}]$ is covered by ten B-spline functions. Therefore, the approximate solution and their derivatives over the element $[x_r,x_{r+1}]$ can be written as

$$\begin{aligned}
U_r &= \delta_{r-4}+502\delta_{r-3}+14608\delta_{r-2}+88234\delta_{r-1}+156190\delta_r\\
&\quad +88234\delta_{r+1}+14608\delta_{r+2}+502\delta_{r+3}+\delta_{r+4},\\
U_r' &= \frac{9}{h}\left(-\delta_{r-4}-246\delta_{r-3}-4046\delta_{r-2}-11326\delta_{r-1}\right.\\
&\quad \left.+11326\delta_{r+1}+4046\delta_{r+2}+246\delta_{r+3}+\delta_{r+4}\right),\\
U_r'' &= \frac{72}{h^2}\left(\delta_{r-4}+118\delta_{r-3}+952\delta_{r-2}+154\delta_{r-1}-2450\delta_r\right.\\
&\quad \left.+154\delta_{r+1}+952\delta_{r+2}+118\delta_{r+3}+\delta_{r+4}\right),\\
U_r''' &= \frac{504}{h^3}\left(-\delta_{r-4}-54\delta_{r-3}-134\delta_{r-2}+434\delta_{r-1}-434\delta_{r+1}\right.\\
&\quad \left.+134\delta_{r+2}+54\delta_{r+3}+\delta_{r+4}\right),\\
U_r^{(4)} &= \frac{3024}{h^4}\left(\delta_{r-4}+22\delta_{r-3}-32\delta_{r-2}-86\delta_{r-1}+190\delta_r\right.\\
&\quad \left.-86\delta_{r+1}-32\delta_{r+2}+22\delta_{r+3}+\delta_{r+4}\right),\\
U_r^{(5)} &= \frac{15120}{h^5}\left(-\delta_{r-4}-6\delta_{r-3}+34\delta_{r-2}-46\delta_{r-1}\right.\\
&\quad \left.+46\delta_{r+1}-34\delta_{r+2}+6\delta_{r+3}+\delta_{r+4}\right),\\
U_r^{(6)} &= \frac{60480}{h^6}\left(\delta_{r-4}-2\delta_{r-3}-8\delta_{r-2}+34\delta_{r-1}-50\delta_r\right.\\
&\quad \left.+34\delta_{r+1}-8\delta_{r+2}-2\delta_{r+3}+\delta_{r+4}\right),\\
U_r^{(7)} &= \frac{181440}{h^7}\left(-\delta_{r-4}+6\delta_{r-3}-14\delta_{r-2}+14\delta_{r-1}\right.\\
&\quad \left.-14\delta_{r+1}+14\delta_{r+2}-6\delta_{r+3}+\delta_{r+4}\right),\\
U_r^{(8)} &= \frac{362880}{h^8}\left(\delta_{r-4}-8\delta_{r-3}+28\delta_{r-2}-56\delta_{r-1}\right.\\
&\quad \left.+70\delta_r-56\delta_{r+1}+28\delta_{r+2}-8\delta_{r+3}+\delta_{r+4}\right).
\end{aligned} \tag{2.4}$$

Using (2.4) in (2.2), a fully-discretized form of the (1.3) is obtained by the CM as

$$\begin{aligned} & (1-\gamma_1)\,\delta_{r-4}^{s+1}+(502-\gamma_2)\,\delta_{r-3}^{s+1}+(14608-\gamma_3)\,\delta_{r-2}^{s+1}+(88234-\gamma_4)\,\delta_{r-1}^{s+1}+156190\delta_r^{s+1} \\ & +(88234+\gamma_4)\,\delta_{r+1}^{s+1}+(14608+\gamma_3)\,\delta_{r+2}^{s+1}+(502+\gamma_2)\,\delta_{r+3}^{s+1}+(1+\gamma_1)\,\delta_{r+4}^{s+1} \\ = \; & (1+\gamma_1)\,\delta_{r-4}^{s}+(502+\gamma_2)\,\delta_{r-3}^{s}+(14608+\gamma_3)\,\delta_{r-2}^{s}+(88234+\gamma_4)\,\delta_{r-1}^{s}+156190\delta_r^{s} \\ & +(88234-\gamma_4)\,\delta_{r+1}^{s}+(14608-\gamma_3)\,\delta_{r+2}^{s}+(502-\gamma_2)\,\delta_{r+3}^{s}+(1-\gamma_1)\,\delta_{r+4}^{s}\,, \end{aligned} \tag{2.5}$$

where

$$\begin{aligned} \beta_1 &= \frac{9\Delta t}{2h},\beta_2=\frac{257\Delta t}{h^3},\beta_3=-\frac{7560\Delta t}{h^5}, \\ \gamma_1 &= \eta^{s+1}\beta_1+\beta_2+\beta_3,\gamma_2=246\eta^{s+1}\beta_1+54\beta_2+6\beta_3 \\ \gamma_3 &= 4046\eta^{s+1}\beta_1+134\beta_2-34\beta_3,\gamma_4=11326\eta^{s+1}\beta_1-434\beta_2+46\beta_3 \\ \eta^j &= \delta_{r-4}^j+502\delta_{r-3}^j+14608\delta_{r-2}^j+88234\delta_{r-1}^j+156190\delta_r^j \\ & \quad +88234\delta_{r+1}^j+14608\delta_{r+2}^j+502\delta_{r+3}^j+\delta_{r+4}^j, j=s+1,s. \end{aligned}$$

Thus, the system is obtained which has $N+1$ equation and $N+9$ unknowns. With the help of the boundary conditions Eq. (1.5), the parameters $\delta_{-4},\delta_{-3},\delta_{-2},\delta_{-1},\delta_{N+1},\delta_{N+2},\delta_{N+3}$ and δ_{N+4} are eliminated from the system, thus obtaining a solvable $(N+1)\times(N+1)$ matrix system. This system is solved easily using the Matlab packet program. δ^0 is achieved to be start the iteration of the system using the initial (1.4) and boundary conditions (1.5), iteratively the δ^s can be obtained at time $t^s=s\Delta t$.

Since getting an implicit system (2.5) according to the term δ, we used an inner iteration in which before moving the calculation of the next time step approximation for time parameter.

2.2. Nonic B-spline Galerkin Method (M2)

Applying the GM to Eq. (2.2), the following integral equation is obtained

$$\begin{aligned} & \int_c^d \Psi(x)\left[U^{s+1}+\frac{\Delta t}{2}\left(U^{s+1}\left(U_x\right)^{s+1}+\left(U_{xxx}\right)^{s+1}-\left(U_{xxxxx}\right)^{s+1}\right)\right]dx \\ = \; & \int_c^d \Psi(x)\left[U^{s}-\frac{\Delta t}{2}\left(U^{s}\left(U_x\right)^{s}+\left(U_{xxx}\right)^{s}-\left(U_{xxxxx}\right)^{s}\right)\right]dx. \end{aligned} \tag{2.6}$$

Let $\Psi(x)$ which is called as a weight function be chosen as the nonic B-spline B_r^9. Using element trial function (2.3) in Eq. (2.6) over the element $[x_r, x_{r+1}]$, the following fully discretized approximation is obtained

$$\begin{aligned}
&\sum_{j=r-4}^{r+5}\left\{\left(\int_{x_r}^{x_{r+1}} B_i^9 B_j^9 dx\right)\delta_j^{s+1}+\frac{\Delta t}{2}\sum_{k=r-4}^{r+5}\left(\int_{x_r}^{x_{r+1}} B_i^9 B_k^9\left(\delta_k^{n+1}\right)\left(B_j^9\right)' dx\right)\delta_j^{s+1}\right.\\
&\left.+\frac{\Delta t}{2}\left(\int_{x_r}^{x_{r+1}} B_i^9\left(B_j^9\right)''' dx\right)\delta_j^{s+1}+\frac{\Delta t}{2}\left(\int_{x_r}^{x_{r+1}} B_i^9\left(B_j^9\right)^{(5)} dx\right)\delta_j^{s+1}\right\}\\
&-\sum_{j=r-4}^{r+5}\left\{\theta_1\left(\int_0^h T_i T_j d\xi\right)\delta_j^s-\frac{\Delta t}{2}\sum_{k=r-4}^{r+5}\left(\int_{x_r}^{x_{r+1}} B_i^9 B_k^9\left(\delta_k^n\right)\left(B_j^9\right)' dx\right)\delta_j^s\right.\\
&\left.-\frac{\Delta t}{2}\left(\int_{x_r}^{x_{r+1}} B_i^9\left(B_j^9\right)''' dx\right)\delta_j^s-\frac{\Delta t}{2}\left(\int_{x_r}^{x_{r+1}} B_i^9\left(B_j^9\right)^{(5)} dx\right)\delta_j^s\right\},
\end{aligned} \tag{2.7}$$

where i also takes the values $r-4$ to $r+5$. The above equation can be rewritten with the element matrices $\mathbf{A}^e, \mathbf{C}^e$ and $\mathbf{D}^e$ with dimensions 10×10 and the element matrix $\mathbf{B}^e$ with dimension $10\times 10\times 10$, in the matrix form as

$$\left[\mathbf{A}^e+\frac{\Delta t}{2}\left(\mathbf{B}^e\left(\boldsymbol{\delta}^e\right)^{s+1}+\mathbf{C}^e-\mathbf{D}^e\right)\right]\left(\boldsymbol{\delta}^e\right)^{s+1}-\left[\mathbf{A}^e-\frac{\Delta t}{2}\left(\mathbf{B}^e\left(\boldsymbol{\delta}^e\right)^s+\mathbf{C}^e-\mathbf{D}^e\right)\right]\left(\boldsymbol{\delta}^e\right)^s, \tag{2.8}$$

where

$$\begin{aligned}
\left(\boldsymbol{\delta}^e\right)^l &= \left(\delta_{m-4}^l,\ldots,\delta_{m+4}^l\right)^T, l=s,s+1,\\
A_{ij}^e &= \int_{x_r}^{x_{r+1}} B_i^9 B_j^9 dx,\quad B_{ij}^e\left(\boldsymbol{\delta}^e\right)^{s+1}=\int_{x_r}^{x_{r+1}} B_i^9 B_k^9\left(\delta_k^{s+1}\right)\left(B_j^9\right)' dx,\\
C_{ij}^e &= \int_{x_r}^{x_{r+1}} B_i^9\left(B_j^9\right)''' dx,\quad D_{ij}^e=\int_{x_r}^{x_{r+1}} B_i^9\left(B_j^9\right)^{(5)} dx.
\end{aligned}$$

The nonlinear matrix equation is produced by assembling the systems (2.8) over all elements

$$\left[\mathbf{A}+\frac{\Delta t}{2}\left(\mathbf{B}\left(\boldsymbol{\delta}^{s+1}\right)+\mathbf{C}-\mathbf{D}\right)\right]\boldsymbol{\delta}^{s+1}=\left[\mathbf{A}-\frac{\Delta t}{2}\left(\mathbf{B}\left(\boldsymbol{\delta}^s\right)+\mathbf{C}-\mathbf{D}\right)\right]\boldsymbol{\delta}^s, \tag{2.9}$$

where $\boldsymbol{\delta}=\left(\delta_{-4},,\ldots,\delta_{N+4}\right)^T$ and $\mathbf{A},\mathbf{B},\mathbf{C}$ and $\mathbf{D}$ are derived from the corresponding element matrices $\mathbf{A}^e,\mathbf{B}^e,\mathbf{C}^e$ and $\mathbf{D}^e$.

The set of Eq. (2.9) consists of $(N+9)$ equations with $(N+9)$ unknown parameters $(\delta_{-4},\ldots,\delta_{N+4})$. Using the boundary (1.5) and initial (1.4) conditions, the initial vector $\delta^0=(\delta_{-4}^0,\ldots,\delta_{N+4}^0)$ can be found and then the other unknown vectors $\delta^{s+1},(s=1,2,\ldots)$ can be found repeatedly by solving the recurrence relation (2.9) using previous δ^s unknown vectors. Note that since the system (2.9) is an implicit system, an inner iteration algorithm is employed at all time steps.

3. Numerical tests

In this section, the methods that presented in this paper as M1 and M2 are tested to get the numerical solutions including the motion of single solitary wave of the KE, the interaction of the two solitary waves and the wave generation of the KE. The three invariants of the motion for KE are given by [11] as

$$\begin{aligned} I_1 &= \int_{-\infty}^{\infty} u dx, \\ I_2 &= \int_{-\infty}^{\infty} \frac{u^2}{2} dx, \\ I_3 &= \int_{-\infty}^{\infty} \left(\frac{u_x^2 + u_{xx}^2}{2} - \frac{u^3}{6} \right) dx. \end{aligned} \tag{3.1}$$

To calculate approximately these integrals, the trapezoidal rule for the space interval $[c, d]$ at all time steps is used. The accuracy of the method is calculated using the following error norms;

$$\begin{aligned} L_2 &= \sqrt{h \sum_{r=0}^{N} (u_r - U_r)^2}, \\ L_\infty &= \max_r |u_r - U_r|, \end{aligned} \tag{3.2}$$

and the order of convergence is computed by

$$\text{order} = \frac{\log \dfrac{(L_\infty)_{k_r}}{(L_\infty)_{k_{r+1}}}}{\log \dfrac{k_r}{k_{r+1}}}, \tag{3.3}$$

where $(L_\infty)_{k_r}$ is the error norm L_∞ with the steps $k_r = \Delta t_r = h_r$.

3.1. Motion of single solitary wave

The exact solution of the KE which represents a single solitary wave is given as

$$u(x,t) = \frac{105}{169} \text{sech}^4 \left(\frac{1}{2\sqrt{13}} \left[x - \tilde{x}_0 - \frac{36}{169} t \right] \right), \tag{3.4}$$

where $\tilde{x}_0$ depicts the peak position of the initially centered wave. By taking $t = 0$ in the analytical solution (3.4), the initial condition can be obtained as

$$u(x,0) = \frac{105}{169} \text{sech}^4 \left(\frac{1}{2\sqrt{13}} [x - \tilde{x}_0] \right). \tag{3.5}$$

To investigate the propagation of the single solitary wave in the interval $[-40, 60]$ with the time period $0 \le t \le 25$ and the parameters $\tilde{x}_0 = 2$, $h = \Delta t = 1/2^i, i = 1, 2, \ldots, 6$, the initial and numerical solutions at

various times are illustrated in Figure 1 for the M1 and M2. According to the figure we can say that the solitary wave remains its initial form during the running time for both of the methods and propagates towards the right across.

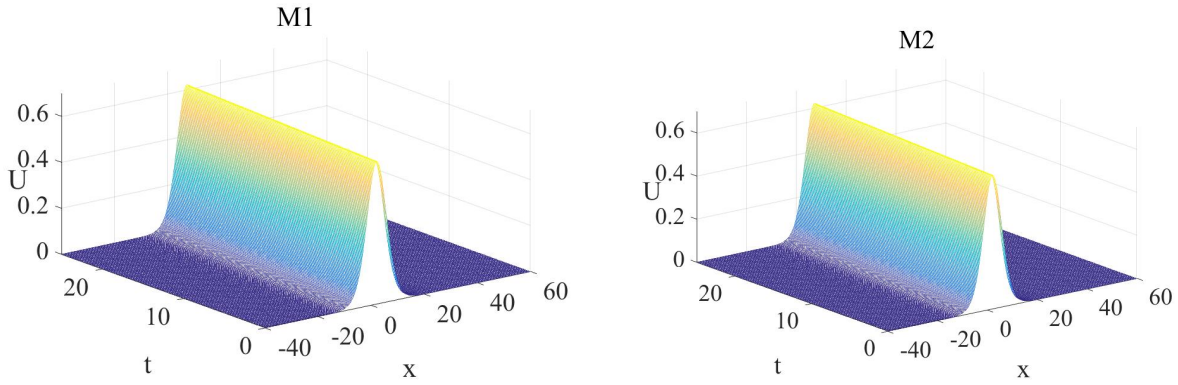

Figure 1. $U(x,t)$ at various times with $h = \Delta t = 0.125$.

The algorithm is run up to time $t = 25$ with the various values for the space and time steps. Table 1 is given the comparison of the obtained error norms L_2 and L_∞ and the conservation invariants for each proposed methods. According to the table, while equal space and time steps are decreased from 1 to 0.03125, all of the error norms L_2 and L_∞ decrease for each proposed methods. When examined Table 1, the numerical values of the conservation invariants also remain almost same with their analytical values and it can be seen that M1 and M2 have nearly same order which is of a quadratic order of convergence. The error norms L_2 and L_∞ are given in Table 2 to compare with the earlier studies in the literature. The methods used in these studies are as the sextic B-spline collocation (SxBSC) [1], the modified cubic B-spline differential quadrature (MCBSDQ) [2], the meshless method of lines with the multiquadric (MQRBF) and Gaussian (GRBF) radial basis functions [4], the meshless method based on collocation with multiquadric (MQRBF-C), the Gaussian (GRBF-C), inversequadric (IQRBF-C) and inverse multiquadric (IMQRBF-C) radial basis functions [6], the radial basis function (RBF)[7], the septic B-spline collocation (SpBSC) [9], the cosine expansion (CDQ) and Lagrange interpolation polynomials (PDQ) based differential quadrature [11] and the multiquadric radial basis functions generated finite difference (MQRDF-FD) [12].

The distribution of the absolute error (analytical - numerical) at time $t = 25$ is demonstrated in Figure 2 for M1 and M2. As carefully inspected from the figures, the maximum error is observed at the middle of the space interval, and this result is also compatible with Table 1.

3.2. Interaction of two solitary waves

In this section, the interaction of two solitary waves having different amplitudes are simulated by using both of the proposed methods M1 and M2 during the time $t = 55$. These solitary waves are obtained by the following initial condition

$$u(x,0) = \sum_{l=1}^{2} \rho_l^2 \operatorname{sech}^4\left(\frac{\sqrt{\alpha\rho_l}}{4}(x - \tilde{x}_l)\right),$$

where

$$\alpha = \frac{4}{\sqrt{105}},\ \rho_l = \frac{\beta_l}{\alpha},\ \beta_l = \frac{12 - 2l}{13},\ \tilde{x}_1 = 0,\ \tilde{x}_2 = 20.$$

Table 1. The error norms L_2 and L_∞, the conservation orders and the invariants at time $t = 25$.

M1						
$\Delta t = h$	L_2	L_∞	Order	I_1	I_2	I_3
1	6.21×10^{-4}	2.37×10^{-4}	2.000	5.973693818	1.272503928	–0.1645866757
0.5	1.56×10^{-4}	5.92×10^{-5}	1.999	5.973690397	1.272503039	–0.1645864969
0.25	3.90×10^{-5}	1.48×10^{-5}	1.999	5.973693139	1.272502959	–0.1645864808
0.125	9.73×10^{-6}	3.71×10^{-6}	2.000	5.973694084	1.272502954	–0.1645864798
0.0625	2.43×10^{-6}	9.26×10^{-7}	2.000	5.973694337	1.272502954	–0.1645864797
0.03125	6.08×10^{-7}	2.31×10^{-7}		5.973694402	1.272502954	–0.1645864798
M2						
1	6.24×10^{-4}	2.32×10^{-4}	1.958	5.973536613	1.272494212	–0.1645845224
0.5	1.56×10^{-4}	5.98×10^{-5}	2.008	5.973674460	1.272502055	–0.1645862720
0.25	3.90×10^{-5}	1.49×10^{-5}	2.004	5.973691858	1.272502881	–0.1645864625
0.125	9.73×10^{-6}	3.71×10^{-6}	2.000	5.973693991	1.272502948	–0.1645864784
0.0625	2.43×10^{-6}	9.26×10^{-7}	2.001	5.973694332	1.272502954	–0.1645864797
0.03125	6.03×10^{-7}	2.32×10^{-7}		5.973694438	1.272502967	–0.1645864825
Exact				5.973695221	1.272565685	–0.1645864798

Table 2. The error norms L_2 and L_∞ at time $t = 25$.

Method	h	Δt	L_2	L_∞
M1	0.1	0.1	6.28×10^{-6}	2.37×10^{-6}
	0.1	0.01	6.24×10^{-8}	2.35×10^{-8}
	0.1	0.001	2.94×10^{-9}	9.35×10^{-10}
M2	0.1	0.1	6.28×10^{-6}	2.37×10^{-6}
	0.1	0.01	6.25×10^{-8}	2.37×10^{-8}
	0.1	0.001	2.89×10^{-9}	8.62×10^{-10}
SxBSC [1]	1	0.01	3.32×10^{-5}	1.56×10^{-5}
MCBSDQ[2]	51/91	0.01	7.2×10^{-5}	2.9×10^{-5}
MQRBF[4]	1	0.01	1.68×10^{-4}	4.66×10^{-5}
GRBF[4]	1	0.01	1.32×10^{-4}	3.99×10^{-5}
MQRBF-C[6]	1	0.1	1.93×10^{-4}	5.12×10^{-5}
GRBF-C[6]	1	0.1	1.54×10^{-4}	4.31×10^{-5}
IQRBF-C[6]	1	0.1	1.23×10^{-3}	3.76×10^{-4}
IMQRBF-C[6]	1	0.1	2.07×10^{-3}	6.42×10^{-4}
RBF[7]	0.2	0.001	2.39×10^{-5}	9.37×10^{-5}
SpBSC[9]	0.2	0.001	1.40×10^{-4}	5.11×10^{-5}
CDQ[11]	1	0.1	1.59×10^{-4}	7.6×10^{-5}
PDQ [11]	1	0.1	2.85×10^{-3}	8.63×10^{-4}
MQRDF-FD [12]	0.1	0.01	5.08×10^{-5}	

The boundary conditions are taken as zero in the solution domain $[-50, 100]$. The time and space steps are chosen as $\Delta t = 0.01$ and $h = 0.2$. In Figure 3, it is seen that the two solitary waves move to the right until the collision time and then propagate to the right with their initial amplitudes again, with the larger amplitude one coming forward. In Table 3, the invariants for the KE at various times are given to compare with the exact values of it and the results of the earlier studies.

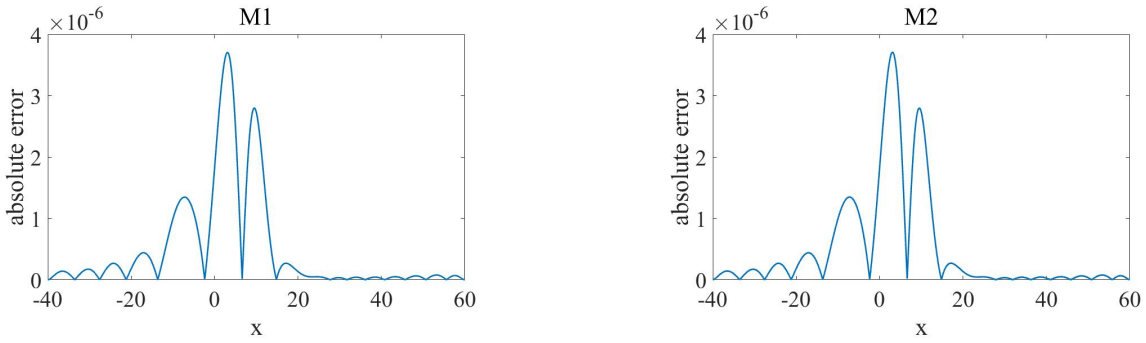

Figure 2. The distribution of the absolute errors for $h = \Delta t = 0.125$.

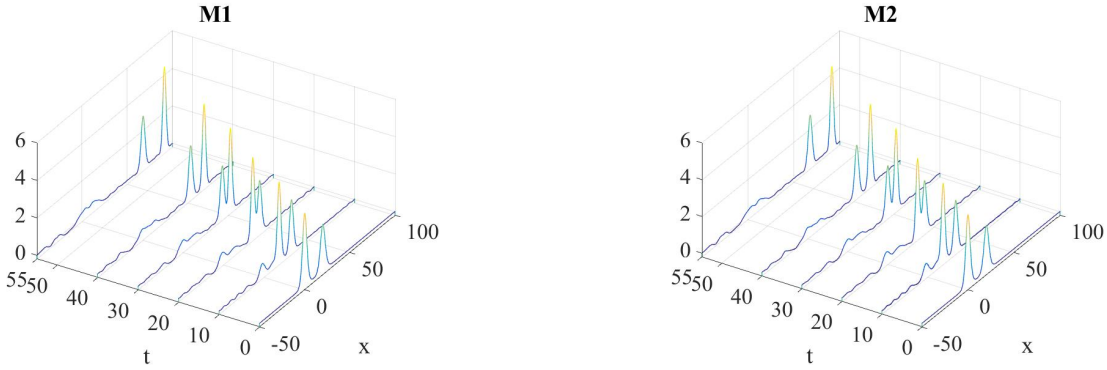

Figure 3. Interaction of two solitary waves at various times.

Table 3. The invariants at the various times.

Method	t	I_1	I_2	I_3
M1	0	40.50926	45.83614	–37.87775
	55	40.52945	45.83604	–37.87540
M2	0	40.50926	45.83614	–37.87775
	55	40.54927	45.84204	–36.98041
MCBSDQ [2]	0	40.50925	45.83613	–37.87775
	55	40.51025	45.83170	–39.53335
MQRBF [4]	0	40.50926	45.83614	–32.37219
	50	40.48389	45.85094	–32.15991
GRBF [4]	0	40.50926	45.83614	–32.37218
	50	40.41284	45.84365	–32.14082
RBF [7]	0	40.50926	45.83614	–32.37218
	55	40.40483	45.83524	–32.37120
SpBSC [9]	0	40.50920	45.83608	–37.87770
	50	40.34304	45.83577	–33.17479
MQRDF-FD [12]	0	40.5093	45.8361	
	55	40.4686	45.8366	
Exact		40.50926	45.83614	–38.85013

3.3. Wave generation

In this numerical test problem, by using the following initial condition we observe the generation of the three solitary waves with the KE.

$$u(x,0) = 10\text{sech}^4\left(\frac{x}{2\sqrt{13}}\right)$$

The boundary conditions are taken as zero in the solution domain $[-20, 100]$. The time and space steps are chosen as $\Delta t = 0.1$ and $h = 0.5$. The algorithms run up to the time $t = 18$. In Figure 4, the generation of the obtained waves are seen for the various times. From the figure, it is seen that the first wave rise in a few time, later the second and third ones are born. At the same time, the first one begins to get its form and then the others too. Finally the obtained three solitary waves get far from eachothers and keep their own shapes.

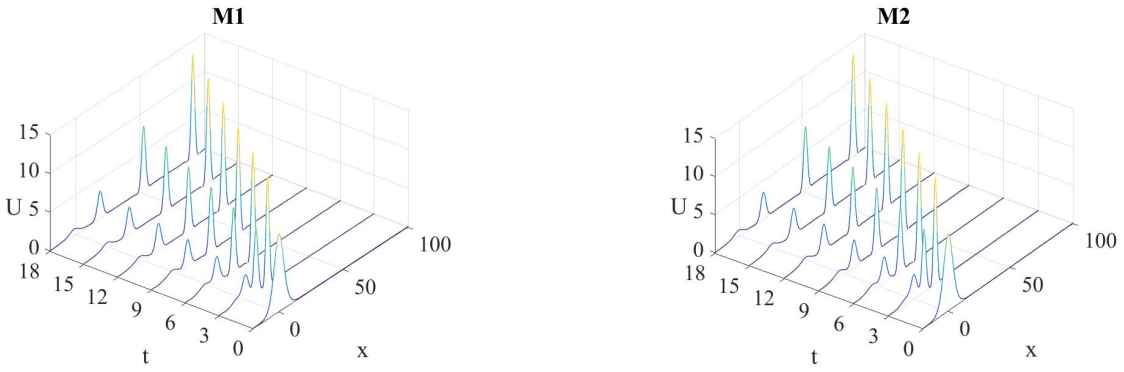

Figure 4. The wave generation of the KE.

4. Conclusion

Using nonic B-spline functions in the collocation and Galerkin finite element methods for space discretization and CNM for time discretization have been proposed to get the numerical solutions for the KE. To see the performance of the proposed methods, the test problems including the motion of the solitary wave, the interaction of the two solitary waves and the wave generation of the KE have been examined. It is seen that the motion of the solitary wave is well simulated by the M1 and M2. For both of the proposed methods the error norms L_2 and L_∞ are considerably smaller than the earlier results. The test problem which includes the interaction of two solitary wave of the KE is shown that the solitary waves keep their shapes after the collision for both of the methods. When the invariant constants, obtained by the M1 and M2 for the second problem, are compared with the exact values of them in the solution domain and with the other studies, it can be said that the compatible results are obtained. Consequently, it is seen from the test problems that the nonic B-spline functions which have not been used before can be used to get the numerical solutions of the high order nonlinear partial differential equations. Considering that it has important geometric properties and low computational costs, it can be said that there are advantages of using B-spline functions as the base function in numerical solution methods.

References

[1] Bagherzadeh AS. B-Spline collocation method for numerical solution of nonlinear kawahara and modified kawahara equations. TWMS Journal of Applied and Engineering Mathematics 2017; 7 (2): 188-199.

[2] Başhan A. An efficient approximation to numerical solutions for the Kawahara equation via modified cubic B-spline differential quadrature method. Mediterranean Journal of Mathematics 2019; 16 (14). doi: 10.1007/s00009-018-1291-9

[3] Başhan A. Highly efficient approach to numerical solutions of two different forms of the modified Kawahara equation via contribution of two effective methods. Mathematics and Computers in Simulation 2021; 179: 111-125. doi: 10.1016/j.matcom.2020.08.005

[4] Bibi N, Tirmizi S, Haq S. Meshless method of lines for numerical solution of Kawahara type equations. Applied Mathematics 2011; 2 (5): 608-618. doi: 10.4236/am.2011.25081

[5] De Boor C. A practical guide to splines. Springer-Verlag, Berlin, 1978.

[6] Dereli Y, & Dağ I. Numerical solutions of the Kawahara type equations using radial basis functions. Numerical Methods for Partial Differential Equations 2012; 28 (2): 542-553. doi: 10.1002/num.20633

[7] Haq S, Uddin M. RBFs approximation method for Kawahara equation. Engineering Analysis with Boundary Elements 2011; 35 (3): 575-580. doi: 10.1016/j.enganabound.2010.07.009

[8] Hunter JK, Scheurle J. Existence of perturbed solitary wave solutions to a model equation for water waves. Physica D Nonlinear Phenomena 1988; 32 (2): 253-268. doi: 10.1016/0167-2789(88)90054-1

[9] Karakoç SBG, Ak T, Zeybek H. Numerical solutions of the Kawahara equation by the septic B spline collocation method. Statistics, Optimization & Information Computing 2014; 2 (3): 211-221. doi: 10.19139/soic.v2i3.74

[10] Kawahara R. Oscillatory solitary waves in dispersive media. Journal of the Physical Society of Japan 1972; 33: 260-264. doi: 10.1143/JPSJ.33.260

[11] Korkmaz A, Dağ I. Crank-Nicolson differential quadrature algorithms for the Kawahara equation. Chaos Solutions and Fractals 2009; 42 (1): 65-73. doi: 10.1016/j.chaos.2008.10.033

[12] Rasoulizadeh MN, Rashidinia J. Numerical solution for the Kawahara equation using local RBF-FD meshless method. Journal of King Saud University-Science 2020; 32 (4): 2277-2283. doi: 10.1016/j.jksus.2020.03.001

[13] Schoenberg IJ. Contributions to the problem of approximation of equidistant data by analytic functions, Part A: On the problem of smoothing of graduation, a first class of analytic approximation formulae, Quarterly of Applied Mathematics 1946; 4 (1): 45-99.

[14] Yuan JM, Shen J, Wu J. A dual-Petrov-Galerkin method for the Kawahara-type equations. Journal of Scientific Computing 2008; 34 (1): 48-63. doi: 10.1007/s10915-007-9158-4